

See discussions, stats, and author profiles for this publication at: <https://www.researchgate.net/publication/353244816>

A critical role of nuclear m6A reader YTHDC1 in leukemogenesis by regulating MCM complex-mediated DNA replication

Article in *Blood* · July 2021

DOI: 10.1182/blood.2021011707

CITATIONS

25

READS

565

16 authors, including:



Yue Sheng

University of Florida

43 PUBLICATIONS 1,525 CITATIONS

[SEE PROFILE](#)



Jiangbo Wei

University of Chicago

30 PUBLICATIONS 2,727 CITATIONS

[SEE PROFILE](#)



Fang Yu

University of Florida

8 PUBLICATIONS 110 CITATIONS

[SEE PROFILE](#)



Yu C.J.

University of Florida

16 PUBLICATIONS 156 CITATIONS

[SEE PROFILE](#)

Some of the authors of this publication are also working on these related projects:



MiR-9 upregulation leads to inhibition of erythropoiesis by repressing FoxO3 Article [View project](#)



oncolytic therapy [View project](#)



American Society of Hematology
2021 L Street NW, Suite 900,
Washington, DC 20036
Phone: 202-776-0544 | Fax 202-776-0545
editorial@hematology.org

A Critical Role of Nuclear m⁶A Reader YTHDC1 in Leukemogenesis by Regulating MCM Complex-Mediated DNA Replication

Tracking no: BLD-2021-011707R2

Yue Sheng (University of Florida, United States) Jiangbo Wei (Howard Hughes Medical Institute, United States) Fang Yu (University of Florida, United States) Huanzhou Xu (College of Medicine University of Florida, United States) Chunjie Yu (University of Florida, United States) Qiong Wu (University of Florida, United States) Yin Liu (University of Florida, United States) Lei Li (Shenzhen Bay Laboratory, China) Xiao-long Cui (Howard Hughes Medical Institute, United States) Xueying Gu (Nanjing Medical University, China) Bin Shen (Nanjing Medical University, China) Wei Li (University of California, Irvine, United States) Yong Huang (University of Virginia, United States) Sumita Bhaduri-McIntosh (University of Florida, United States) Chuan He (Howard Hughes Medical Institute, United States) Zhijian Qian (University of Florida, United States)

Abstract:

YTHDC1 has distinct functions as a nuclear N⁶-methyladenosine (m⁶A) reader in regulating RNA metabolism. Here we show that *YTHDC1* is overexpressed in Acute Myeloid Leukemia (AML) and that it is required for proliferation and survival of human AML cells. Genetic deletion of *Ythdc1* markedly blocks AML development and maintenance as well as self-renewal of leukemia stem cells (LSCs) *in vivo* in mice. We find that *Ythdc1* is also required for normal hematopoiesis and hematopoietic stem/progenitor cell (HSPC) maintenance *in vivo*. Notably, *Ythdc1* haploinsufficiency reduces self-renewal of LSCs, but not HSPCs *in vivo*. *YTHDC1* knockdown has a strong inhibitory effect on proliferation of primary AML cells. Mechanistically, YTHDC1 regulates leukemogenesis through MCM4, which is a critical regulator of DNA replication. Our study provides the compelling evidence to show an oncogenic role and a distinct mechanism of YTHDC1 in AML.

Conflict of interest: COI declared - see note

COI notes: C.H. is a scientific founder and a scientific advisory board member of Accent Therapeutics, Inc. and a shareholder of Epican Genentech. Other authors declare no potential conflicts of interest.

Preprint server: No;

Author contributions and disclosures: Z.Q. and C.H. conceived the project and designed the experiments. Y.S., J.W., F.Y., H.X., C.Y., Q.W., Y.L. performed experiments; Z.Q., Y.S., H.X., Y. W., L.L. and X.C. analyzed data; Z.Q. and Y.S. wrote the manuscript; B.S., X.G., W.L. and S.B.M. provided advice and new reagents/analytic tools and all authors provided critical review of the manuscript.

Non-author contributions and disclosures: No;

Agreement to Share Publication-Related Data and Data Sharing Statement: RNA-seq data have been deposited in NCBI Gene Expression Omnibus (GEO) database under accession number GSE178859.

Clinical trial registration information (if any):

A Critical Role of Nuclear m⁶A Reader YTHDC1 in Leukemogenesis by Regulating MCM Complex-Mediated DNA Replication

Yue Sheng^{1,10}, Jiangbo Wei^{2,3,10}, Fang Yu¹, Huanzhou Xu⁴, Chunjie Yu¹, Qiong Wu¹, Yin Liu¹, Lei Li^{5,6}, Xiao-long Cui^{2,3}, Xueying Gu⁷, Bin Shen⁷, Wei Li⁵, Yong Huang⁸, Sumita Bhaduri-McIntosh^{4,9}, Chuan He^{2,3*} and Zhijian Qian^{1*}

¹Department of Medicine, UF Health Cancer Center, University of Florida, Gainesville, FL 32610.

² Department of Chemistry, Department of Biochemistry and Molecular Biology, and Institute for Biophysical Dynamics, The University of Chicago, 929 East 57th Street, Chicago, IL 60637.

³ Howard Hughes Medical Institute, The University of Chicago, 929 East 57th Street, Chicago, IL 60637.

⁴ Division of Infectious Disease, Department of Pediatrics, University of Florida, Gainesville, FL, U.S.A.

⁵ Department of Biological Chemistry, School of Medicine, University of California, Irvine, 5270 California Ave, Irvine CA, 92617

⁶Institute of Systems and Physical Biology, Shenzhen Bay Laboratory, Shenzhen, 518107, China

⁷State Key Laboratory of Reproductive Medicine, Center for Global Health, Gusu School, Women's Hospital of Nanjing Medical University, Nanjing Maternity and Child Health Care Hospital, Nanjing Medical University, Nanjing 211166, China

⁸Department of Medicine, University of Virginia, Charlottesville, VA

⁹ Department of Molecular Genetics and Microbiology, University of Florida, Gainesville, FL, U.S.A.

¹⁰Equal contribution

*Correspondence:

chuanhe@uchicago.edu

Zhijian.Qian@medicine.ufl.edu

Lead contact: Zhijian Qian

Abstract

YTHDC1 has distinct functions as a nuclear N^6 -methyladenosine (m^6A) reader in regulating RNA metabolism. Here we show that *YTHDC1* is overexpressed in Acute Myeloid Leukemia (AML) and that it is required for proliferation and survival of human AML cells. Genetic deletion of *Ythdc1* markedly blocks AML development and maintenance as well as self-renewal of leukemia stem cells (LSCs) *in vivo* in mice. We find that *Ythdc1* is also required for normal hematopoiesis and hematopoietic stem/progenitor cell (HSPC) maintenance *in vivo*. Notably, *Ythdc1* haploinsufficiency reduces self-renewal of LSCs, but not HSPCs *in vivo*. *YTHDC1* knockdown has a strong inhibitory effect on proliferation of primary AML cells. Mechanistically, YTHDC1 regulates leukemogenesis through MCM4, which is a critical regulator of DNA replication. Our study provides the compelling evidence to show an oncogenic role and a distinct mechanism of YTHDC1 in AML.

Key Points:

- YTHDC1 is critical for normal and malignant hematopoiesis.
- The YTHDC1/ m^6A /MCM4/DNA replication axis plays a pivotal role in leukemogenesis.

Introduction:

N⁶-methyladenosine (m⁶A) is one of the most prevalent modifications of mammalian mRNA^{1,2}. m⁶A regulates multiple stages of mRNA metabolism, including RNA folding, maturation, nuclear processing, and export, as well as mRNA translation and stability³⁻⁵. RNA m⁶A modification is dynamically controlled by a methyltransferase complex (writer) and m⁶A demethylases (erasers)^{1,4,5}. m⁶A-sites can be recognized by a number of RNA binding proteins, which serve as m⁶A readers, and are the functional mediators of m⁶A⁶⁻¹¹. YT521-B homology (YTH) domain family of proteins (YTHDF1, 2, 3, YTHDC2), insulin-like growth factor 2 mRNA-binding protein IGF2BPs (IGF2BP1, 2, 3), and proline-rich and coiled-coil-containing protein 2A (PRRC2A) are cytoplasmic proteins that bind preferentially to m⁶A-modified mRNA, which affects the stability and translation of mRNAs^{7,8,11,12}. A few nuclear RNA readers including heterogeneous nuclear ribonucleoproteins A2/B1 (HNRNPA2B1) and YTHDC1 were identified¹³. As the only YTH domain family member acting as a direct nuclear RNA m⁶A reader, YTHDC1 has distinct roles in regulating nuclear RNA splicing, alternative polyadenylation, nuclear export and decay in an m⁶A-dependent manner¹⁴⁻¹⁷.

mRNA methylation has substantial roles in the regulation of cellular transitions between distinct states during development and differentiation¹⁸. Tight regulation of m⁶A RNA modification is critical for normal hematopoiesis^{19,20}. Both Mettl3 and Mettl14 are required for HSC maintenance^{21 22 23}. As an m⁶A reader, Ythdf2 plays a critical role in the maintenance of HSCs by regulating the decay of transcripts responsible for HSC self-renewal.

Knockout (KO) of *Ythdf2* leads to expansion of functional HSCs²⁴⁻²⁶. Notably, *Alkbh5* loss only has a slight effect on HSC self-renewal under stress conditions²⁷.

Dysregulation of dynamic m⁶A methylation contributes to the cancer initiation, development, and maintenance as well as cancer metastasis and relapse²⁸. In AML patients, METTL3 and METTL14 are upregulated, and are required for AML cell survival and leukemia progression by inducing m⁶A deposition of its associated mRNAs²⁹⁻³¹. Interestingly, both FTO and ALKBH5 RNA demethylases are also upregulated in AML patients and promote leukemogenesis^{27,32}. *Ythdf2* as an m⁶A reader is critical for LSC maintenance and AML development²⁵. However, as a nuclear RNA reader, the precise role of YTHDC1 in leukemogenesis and normal hematopoiesis remains unknown. In this study, we thoroughly examined the role and mechanism of YTHDC1 as a nuclear m⁶A RNA reader in normal and malignant hematopoiesis.

Methods

Mice

Ythdc1^{fl/fl} mice³³ were mated to Mx1-Cre transgenic mice³⁴ to generate Ythdc1^{fl/+} Mx1Cre and Ythdc1^{fl/fl} Mx1Cre mice. Ythdc1^{fl/fl} mice were generated from Ythdc1^{fl/fl} chimeric mice crossing with flipper mice to excise the FRT flanked selection cassette³³. All animal research was approved by the University of Florida Institutional Animal Care and Use Committee (Protocol # 201810191).

Cell culture

All cell lines were purchased from ATCC or DSMZ. CD34⁺ cells were purified from the umbilical cord blood. All patient samples were collected under University of Florida Institutional Review Board policies and protocols (IRB#201800547), karyotype information is listed in Supplemental Table 1.

Plasmid construction, retroviral infection and colony forming assay

Human YTHDC1 wildtype and mutant (W377A W428A)¹⁵ were cloned into PCDH vector and pLIX-402 inducible vector (Addgene # 41394). shRNA constructions were described in supplemental methods. Retroviral infection of hematopoietic cells and colony forming assay of mouse HSPCs, human CD34⁺ as well as primary AML patient samples were performed as we previously described^{35 36}.

Transplantation

Leukemia cell transplantation and competitive repopulation were performed as we described in our previous manuscript³⁷ and supplemental methods.

Flow cytometric analysis

Leukemia stem cell and HSPC population staining, in vivo BrdU, HSPC quiescence as well as apoptosis assay were performed as we previously described^{36,38}. All cells were analyzed by flow cytometry on CytoFLEX S or CyAn bench-top analyzer (Beckman Coulter).

RNA-seq and RT-PCR analysis

Cells were harvested and RNA was extracted. Libraries were constructed and subjected to Illumina sequencers by Novogene company. Quantitative Real-Time PCR (qRT-PCR) was performed on QS3 0.2ML QPCR SYSTEM (Thermo Fisher). All primers are listed in Supplemental Table 2, part of them are from Primer Bank³⁹.

MeRIP-RT-qPCR and RIP-RT-qPCR Analysis

MeRIP analysis was performed according to the published paper⁴⁰. And m⁶A enrichment was determined by qRT-PCR analysis. RIP-RT-qPCR was performed as we previously described³⁵.

RNA stability Assay

Cells were cultured in medium with 5 µg/ml actinomycin D and harvested at indicted time points, which results in transcription inhibition. Genes' expression was examined by

RT-qPCR and half-life was analyzed by GraphPad Prism5.

Polysome Profiling Assay

Polysome profiling was performed as reported previously⁸.

DNA Fiber Analysis

DNA fiber analysis was performed as previously described⁴¹. The details are described in supplemental data. The images of DNA fibers were acquired with fluorescence microscope (OLYMPUS) equipped with the OLYMPUS U-TV0.63XC digital camera and analyzed with Image J software⁴².

Quantification And Statistical Analysis

Statistical significance was calculated using the two tailed Student's t test. Results are expressed as the mean \pm standard deviation (SD) for at least triplicate experiments. P values were calculated by Microsoft Excel or GraphPad Prism5, p value of < 0.05 was regarded as statistically significant. Kaplan-Meier survival curve was generated by GraphPad Prism5.

Data Availability

RNA-seq data have been deposited in NCBI Gene Expression Omnibus (GEO) database under accession number GSE178859.

Results:

YTHDC1 Is Highly Expressed In AML.

To determine the role of YTHDC1 in AML, we first examined the YTHDC1 expression level in two independent datasets obtained from websites, GEPIA2⁴³ and Bloodspot⁴⁴. As compared to healthy donor cells, YTHDC1 shows significantly higher expression in AML cells (Figure 1A). In addition, we observed that YTHDC1 was expressed at a significantly higher level in various subtypes of AML compared to normal hematopoietic stem cell (HSC) controls (Figure 1B). Western blot and qRT-PCR showed that YTHDC1 exhibits ectopic high expression level in AML cells compared to CD34⁺ cells derived from healthy donors (Figure 1C; supplemental Figure 1A). However, YTHDC1 overexpression is not associated with a poor survival in AML patients ($p=0.22$)⁴³.

YTHDC1 Is Required For Proliferation And Survival Of Human AML Cells *in vitro*.

To determine the effects of YTHDC1 inhibition on human AML cell proliferation and survival, we knocked down YTHDC1 using YTHDC1-specific shRNAs in human AML cells including NB-4, KASUMI-1 and MOLM-13 cells, which are three common AML subtypes with abnormal cytogenetics: t(15;17), t(8;21) and t(11q23), respectively.

As determined by western blot, YTHDC1-specific shRNAs (Ysh1#, Ysh2#) inhibited YTHDC1 expression in all three tested cell lines (Figure 1D). The results showed that YTHDC1 knockdown (KD) led to a substantially suppressed cell growth of AML cells and induced their apoptosis (Figure 1E-H; supplemental Figure 1B). Consistently, colony-forming ability of the AML cells with YTHDC1 KD was notably decreased (Figure 1I; supplemental

Figure 1C-E). Interestingly, differentiated cells, as determined by CD11b⁺ and CD14⁺, were accumulated after YTHDC1 KD (Figure 1J-L; supplemental Figure 1F). Notably, forced expression of YTHDC1 wildtype (YC1-wt), but not YTHDC1^{W377A/W428A} (YC1-m), a mutant that has a markedly reduced m⁶A-binding ability¹⁵ by an inducible or non-inducible lentiviral vector, promoted cell growth and colony-forming ability of MOLM-13 and KASUMI-1 AML cells (supplemental Figure 1G-N). These data indicate that YTHDC1 promotes human AML cell growth in an m⁶A-dependent manner.

YTHDC1 Is Required For Leukemogenesis In Mice.

To comprehensively understand the role of *Ythdc1* in leukemogenesis, oncogenes were introduced to transform the Lin⁻ BM cells isolated from *Ythdc1*^{fl/+} (WT), *Ythdc1*^{fl/+}Mx1Cre (*Ythdc1* HET), and *Ythdc1*^{fl/fl}Mx1Cre (*Ythdc1* KO). The deletion of *Ythdc1* was induced by three dosages of Polyinosinic: polycytidylic acid (pIpC) injection, which was confirmed by semiquantitative PCR analysis (Figure 2A). Four oncogenes, including MLL-AF9 (generated by t(11q23) translocation), AML1-ETO9a (generated by t(8;21) translocation) and PML-Rara (generated by t(15;17) translocation) as well as HOXA9 which is highly expressed in more than 50% AML⁴⁵, were expressed by MSCV retroviral vectors at comparable levels in WT, HET and KO cells (supplemental Figure 2 A-D). *Ythdc1* expression was confirmed in MLL-AF9 transformed WT, HET and KO cells (supplemental Figure 2 E-F). Compared to transformed WT bone marrow (BM) cells, *Ythdc1* HET and KO BM cells expressing oncogenes had a significantly lower cell growth rate in a dose-dependent manner (Figure 2B-E). While oncogene-transformed *Ythdc1* HET BM cells formed fewer colonies with a

smaller size compared to the colonies generated by oncogene-transformed WT BM cells (Figure 2F-G; supplemental Figure 2G-I), oncogene-transformed *Ythdc1* KO BM cells almost lost their abilities to generate colonies (Figure 2F-G; supplemental Figure 2G-I). Genotyping showed that colonies derived from *Ythdc1* KO BM cells escaped from excision induced by pIpC (Supplemental Figure 2J).

To elucidate *Ythdc1* function *in vivo*, MLL-AF9 (MA9)-WT, *Ythdc1* HET, and *Ythdc1* KO BM cells were transplanted into sub-lethally irradiated recipient C57BL/6 mice. As determined by flow cytometric analysis of peripheral blood (PB), *Ythdc1* KO significantly inhibited AML cell growth *in vivo* (Figure 2H), and the recipient mice showed normal white blood counts (WBC) (Figure 2I) after one-month post transplantation. No differences were observed among WT and HET recipient mice (Figure 2H-I). All MA9-WT and HET recipient mice died within 80 days (Figure 2J) with AML blast cell infiltration in PB, liver, and spleen (Figure 2K). None of the MA9-KO recipient mice died within 100 days (Figure 2J) and no AML blast cells were detected in PB, liver, and spleen from these mice (Figure 2K), and no hepatosplenomegaly was observed (supplemental Figure 2K-L). These data indicate that *Ythdc1* is required for leukemogenesis.

We next evaluated the effects of *Ythdc1* loss on established MA9-transformed leukemia *in vivo*. We expressed an inducible Cre-estrogen receptor (ER) fusion protein (Cre-ER)⁴⁶ in MA9 *Ythdc1*^{fl/fl} BM cells, followed by transplantation into recipient C57BL/6 mice. Induction of *Ythdc1* deletion by 4-OHT treatment, which resulted in significant decrease of *Ythdc1*

expression, markedly inhibited proliferation and colony-forming ability of Cre-ER-MA9-*Ythdc1*^{fl/fl} BM cells while no influence was observed in MA9-*Ythdc1*^{fl/fl} cells with 4-OHT treatment (supplemental Figure 3 A-F). However, no obvious *Ythdc1* deletion was detected by PCR analysis of genomic DNA from the 4-OHT treated Cre-ER-MA9-*Ythdc1*^{fl/fl} BM cell colonies, indicating that the cells escaped from *Ythdc1* excision dominated the cell population after first plating (supplemental Figure 3G).

To perform the *in vivo* experiments, Cre-ER-MA9-*Ythdc1*^{fl/fl} cells were transplanted into sub-lethally irradiated C56BL/B6 recipient mice. When the AML was onset (leukemia cells >10% in peripheral blood) in recipient mice, the mice were administered by Tamoxifen (TAM) or vehicle control. After one-month post TAM treatment, WBC (Figure 2L), BM cellularity (supplemental Figure 3H), and spleen weights (supplemental Figure 3I) were significantly decreased while the frequency of apoptotic BM cells (Figure 2M) was significantly increased in TAM-treated mice compared to vehicle-treated mice. TAM-treated mice had less infiltration in PB and liver and more mature myeloid cells in BM (Figure 2N), as well as more red cells in SP suspension (supplemental Figure 3J). Consistent with these observations, TAM-treated mice had more mature myeloid cells in BM as well as more red cells in BM and SP (supplemental Figure 3K-N). Not surprisingly, AML mice with TAM treatment exhibited longer survival time (Figure 2O). The majority of cells isolated from the moribund TAM-treated mice were WT cells (supplemental Figure 3O), indicating that the cells escaped from excision had a growth advantage, which finally caused the death of mice.

Ythdc1 Maintains Leukemia Stem Cell Pool.

Since MLL-AF9 *Ythdc1* KO BM cells hardly grew *in vitro*, we analyzed MA9-WT and MA9-*Ythdc1* HET BM cells *in vitro*. Loss of one allele of *Ythdc1* reduced Lin⁻ and Lin⁻cKit⁺ cells, which had enriched LSCs *in vitro* (Figure 3A). In addition, an increased rate of apoptosis was detected in MA9-*Ythdc1* HET Lin⁻cKit⁺ cells as compared to MA9-WT Lin⁻cKit⁺ cells (Figure 3B). We next characterized the LSCs in primary recipient mice. As shown in Figure 3C, the leukemic granulocyte-monocyte progenitors (L-GMPs), which represent leukemia stem cells (LSCs) in MA9 leukemia mice⁴⁷, were significantly decreased in MA9-KO but not MA9-HET primary recipient mice compared to MA9-WT recipient mice. G₀ phase of MA9-HET L-GMPs was decreased significantly compared to MA9-WT L-GMPs (Figure 3D-E), suggesting that loss of one allele of *Ythdc1* reduced quiescence of L-GMPs, which may impair LSC function. To further determine the function of MA9-HET LSCs, we performed secondary transplantation of BM cells from MA9-HET and MA9-WT primary recipient mice. Deletion of *Ythdc1* in BM cells from primary MA9-HET recipient mice was confirmed by PCR (supplemental Figure 4A). Six weeks post-transplantation, the recipient mice received MA9-*Ythdc1* HET BM cells had a significantly low white blood counts (WBC) (Figure 3F) and BM cellularity (supplemental Figure 4B) with reduced leukemic burden (Figure 3G) and weights of spleen and liver compared to MA9-WT recipient mice (supplemental Figure 4C-D). L-GMPs and cKit⁺Gr1⁻ cells, which are also considered as LSC-enriched populations⁴⁸, were decreased significantly in MA9-HET recipient mice (Figure 3H-J). MA9-*Ythdc1* HET mice also had more mature myeloid cells in BM and Spleen, red cells in spleen compared to MA9-WT recipient mice (supplemental Figure 4E-H). As

shown in Figure 3K, MA9-*Ythdc1* HET recipient mice had significantly longer survival time compared to MA9-WT mice. These data indicate that loss of one allele of *Ythdc1* significantly impairs the LSC function *in vivo*.

Notably, *Ythdc1* deletion in Cre-ER-MA9-*Ythdc1*^{fl/fl} BM cells by 4-OHT *in vitro* reduced the frequency of Lin⁻ and Lin⁻cKit⁺ cells (supplemental Figure 4I-K) and promoted cell apoptosis (supplemental Figure 4L) and differentiation (supplemental Figure 4M). No influence was observed when MA9-*Ythdc1*^{fl/fl} cells were treated with 4-OHT (supplemental Figure 4N-Q), ruling out the possibility that 4-OHT affected the cell status. Additionally, we found that TAM treated mice have less L-GMPs and cKit⁺Gr1⁻ cells as compared to vehicle-treated recipient mice (Figure 3L-M). Together, these data suggest that *Ythdc1* is required for the maintenance of MA9-LSC.

***Ythdc1* Is Required For Normal Hematopoiesis And HSC Maintenance.**

As determined by qRT-PCR, *Ythdc1* has comparable expression level in hematopoietic stem/progenitor cells (HSPCs), and it is expressed at a relatively lower level in myeloid and red cells than it is in B and T cells (supplemental Figure 5A). To determine the *in vivo* function of *Ythdc1* in hematopoiesis, we generated cohorts of mice including *Ythdc1*^{fl/+} (WT), *Ythdc1*^{fl/+}Mx1Cre (*Ythdc1* HET), and *Ythdc1*^{fl/fl}Mx1Cre (*Ythdc1* KO). *Ythdc1* deletion was induced by pIpC and the elimination of *Ythdc1* in *Ythdc1* KO cells was validated by real-time PCR and western blot (supplemental Figure 5B-E). Notably, *Ythdc1* KO mice showed markedly decreased complete blood counts (CBC), including WBC, red blood counts (RBC),

and platelets (PLT) (Figure 4A-D), and all mice died in 3 weeks (Figure 4E). No differences were observed between WT and *Ythdc1* HET mice (Figure 4A-E). Furthermore, the *Ythdc1* KO mice had a markedly lower BM cellularity than WT mice did, whereas *Ythdc1* HET and WT mice had comparable BM cellularity (Figure 4F-G). Mature cells including myeloid, B and T cells, were decreased dramatically in *Ythdc1* KO mice whereas *Ythdc1* HET and WT mice showed comparable number of mature cells (Figure 4H-J). *Ythdc1* KO BM cells but not *Ythdc1* HET BM significantly lost their ability to generate colonies (Figure 4K; supplemental Figure 5F). These data indicate that loss of *Ythdc1* leads to rapid hematopoietic failure, but the haploinsufficiency of *Ythdc1* does not affect normal hematopoiesis.

To investigate the effects of YTHDC1-overexpression on normal HSPCs, we expressed YTHDC1 in Lin⁻ BM cells. As shown in supplemental Figure 5G, YTHDC1-overexpressing HSPCs grew more slowly at the first few days of cell culture compared to vector-overexpressing , but gained significant growth advantage over vector-expressing cells after 8 days in liquid culture. Consistently, serial plating assay showed that YTHDC1 overexpressing HSPCs also gave rise to fewer colonies at 1st plating but significantly more colonies at 3rd plating as compared to vector expressing HSPCs (supplemental Figure 5H). By flow cytometric analysis of the cells collected from 1st plating, we found that YTHDC1 overexpression significantly increased the frequency of Lin⁻cKit⁺ HSPCs and reduced the frequency of mature myeloid cells (supplemental Figure 5I-J). These data indicate that YTHDC1 overexpression blocks differentiation and increases proliferation/self-renewal of HSPCs, supporting an oncogenic role of YTHDC1 in HSPCs.

As expected, *Ythdc1* KO mice but not *Ythdc1* HET mice displayed much lower number and frequency of hematopoietic progenitor cell (HPC), Lin⁻Sca1⁺cKit⁺(LSK) and HSC compared to WT mice (Figure 4L-N; supplemental Figure 5K-L). Two days after induction of *Ythdc1* deletion by pIpC, the frequency of apoptosis was significantly increased in HSCs, LSKs and HPCs but not Lin⁻ from *Ythdc1* KO mice compared with *Ythdc1* control mice (supplemental Figure 5M). However, we failed to detect HSC population 8 days after induction of *Ythdc1* deletion by pIpC, indicating that *Ythdc1* loss leads to a rapid exhaustion of HSCs (supplemental Figure 5M). Additionally, we introduced an inducible ER Cre into *Ythdc1*^{fl/fl} BM cells in vitro. Induction of *Ythdc1* deletion by 4-OHT significantly increased the frequency of apoptosis of LSK and HSC (supplemental Figure 5N). These data suggest that *Ythdc1* is required for HSPC survival.

To investigate whether *Ythdc1* loss impairs HSC function *in vivo*, we performed the serial competitive repopulation assay. pIpC was administrated one-month after 1st transplantation, 2nd transplantation was performed 4 months after pIpC injection. Before pIpC treatment, the donor-derived cells from WT, *Ythdc1* HET, and KO BM cells (CD45.2⁺) showed similar percentage with WT competitor-derived cells (CD45.1⁺CD45.2⁺) in PB from recipient mice (supplemental Figure 5O). After pIpC administration, percentage of *Ythdc1* KO donor-derived cells but not *Ythdc1* HET donor-derived cells was significantly decreased after 1st and 2nd transplantation (Figure 4O; supplemental Figure 5O). *Ythdc1* KO HSPCs had a significant decrease of repopulation ability in all three lineages including myeloid, B and T cells (Figure 4P). In addition, further analysis of percentage of donor-derived cells in

subpopulations of BMs in the 1st and 2nd round of recipient mice revealed that *Ythdc1* KO HSPCs gave rise to a significantly lower number of LT-HSCs and all subpopulations of myeloid progenitor cells and mature cells than *Ythdc1* HET and WT HSPCs (Figure 4Q). We showed that all generated colonies (Figure 2F and 4K) derived from *Ythdc1* KO cells on the 1st plating were escaped from pIpC induced deletion (Figure S2J and data not shown). Thus, the detected HSCs derived from donor KO mice in the recipient mice are likely escaped from *Ythdc1* excision (Fig. 4Q). These data suggest that *Ythdc1* KO but not *Ythdc1* haploinsufficiency has a significantly negative impact on HSC maintenance.

***Ythdc1* Regulates HSC Function In An Intrinsic Manner.**

To determine whether *Ythdc1* regulates HSC function in an intrinsic or extrinsic manner, we transplanted BM cells (CD45.2⁺) from WT, *Ythdc1* HET, and *Ythdc1* KO mice without pIpC treatment into lethally irradiated syngeneic WT recipients (CD45.1⁺). After one-month post transplantation, *Ythdc1* deletion was induced by pIpC administration. The recipient mice reconstituted *Ythdc1* KO BM cells rapidly developed BM failure, as evidenced by a significant decrease of hematopoietic parameters (supplemental Figure 6A-D) as well as BM cellularity (supplemental Figure 6E) and all mice died within 5 weeks while *Ythdc1* HET and WT recipient mice survived well (supplemental Figure 6F). HPCs, LSKs and HSCs as well as mature myeloid and B cells were all decreased dramatically in *Ythdc1* KO recipient mice as compared to *Ythdc1* HET and WT recipient mice (supplemental Figure 6G-L), indicating that *Ythdc1* intrinsically regulates hematopoiesis and HSC functions.

YTHDC1 Stabilizes Transcripts Encoding Subunits Of MCM Complex.

We next performed RNA-seq analysis of MOLM-13 AML cells expressing YTHDC1 shRNAs (Ysh1# and Ysh2#) or a non-sense scrambled control shRNA (Scr). We identified 1222 differentially expressed genes (586 up and 636 down) ($p < 0.05$, fold change > 1.5) upon YTHDC1 KD (Figure 5A). Pathway analysis revealed that the enriched gene sets of downregulated genes upon YTHDC1 KD were involved in the regulation of cell cycle, DNA replication, steroid biosynthesis, homologous recombination, and Pyruvate metabolism *etc.* whereas the enriched gene sets of upregulated genes include pathways in lysosome, p53 signaling pathway, and apoptosis *etc.* (Figure 5B-C). Among these genes, 265 genes have at least one m⁶A site in MOLM-13 cells^{29,31,49} with potential YTHDC1 binding sites according to published databases^{15,50} (Figure 5D). By qRT-PCR analysis, we confirmed that MCM2, 4, 5 and RFC1, as well as CHAF1a, which play an essential role in DNA replication⁵¹⁻⁵⁴, were all significantly downregulated upon YTHDC1 KD in MOLM-13 cells (Figure 5E). In addition, BCL2 was also markedly down-regulated in YTHDC1 KD MOLM-13 cells (Figure 5E), providing molecular evidence supporting the role of YTHDC1 in regulating proliferation and survival of leukemia cells. MeRIP-qPCR and YTHDC1RIP-qPCR analyses were performed in MOLM13 cells with or without YTHDC1 KD. The results showed that MCM2, MCM4, MCM5 and CHAF1a transcripts are m⁶A-modified, and are directly bound by YTHDC1. YTHDC1 KD did not affect m⁶A modification of MCM2, MCM4, MCM5 and CHAF1a transcripts (Figure 5F-I). These results suggest that YTHDC1 regulates the expression of MCM2, MCM4, MCM5 and CHAF1a genes through binding to the m⁶A sites on these transcripts (Figure 5F-G). However, we did not detect direct binding of YTHDC1 to

BCL2 mRNA, indicating that YTHDC1 may not directly regulate BCL2 expression.

Interestingly, we found that YTHDC1 KD notably reduced the stability of transcripts of MCM2, 4, 5 and CHAF1a (Figure 5J-K; supplemental Figure 7A-B). Analysis of ratio of transcripts in cell nucleus and cytoplasm by qRT-PCR revealed that the expression ratios for nuclear and cytoplasmic MCM4 and MCM5 were not changed after YTHDC1 KD in leukemia cells (supplemental Figure 7C). In addition, we also performed polysome profiling assay in YTHDC1 KD leukemia cells. The results showed that the translation efficiency was not affected by YTHDC1 KD (supplemental Figure 7D-G). These data showed that YTHDC1 does not regulate exportation out of the nucleus as well as translation of MCM4 and MCM5 in leukemia cells.

MCM4 mRNA Is A Key Downstream Effector Of YTHDC1 In Regulating Leukemogenesis.

Analysis of public database⁴⁴ shows that MCM4 is highly expressed in various subtypes of AML compared to normal HSC controls (Figure 6A). MCM4 expression level correlates with YTHDC1 expression level ($P < 0.003$) in AML patients (supplemental Figure 8A). In addition, we showed that YTHDC1 KD resulted in downregulation of MCM4 in primary leukemia cells from AML patients (supplemental Figure 8B). To determine whether MCM4 serves as an important downstream effector of YTHDC1 in leukemogenesis, we examined the consequences of MCM4 KD in AML cells. Similar to YTHDC1 KD, MCM4 KD by MCM4 specific shRNAs (supplemental Figure 8C) suppressed cell growth and colony-forming ability, while promoted cell apoptosis and differentiation of MOLM-13 cells (Figure 6B-E).

Notably, forced expression of YTHDC1 markedly upregulated MCM4 expression whereas YTHDC1^{W377A/W428A} (YC1-m) with a reduced m⁶A binding activity had moderate effect on MCM4 expression in MOLM-13 cells (Figure 6F). In addition, YTHDC1 but not YTHDC1^{W377A/W428A} overexpression significantly increased MCM4 mRNA half-life (Figure 6G), suggesting that YTHDC1 regulates MCM4 expression by stabilizing its mRNA in an m⁶A dependent manner.

To determine whether MCM4 largely mediates YTHDC1 function in AML cells, we expressed MCM4 in YTHDC1 KD MOLM-13 cells using lentivirus. MeRIP assay showed that exogenously expressed MCM4 transcripts had m⁶A modification (supplemental Figure 8D). As shown in Figure 6H-K and supplemental Figure 8E, restoration of MCM4 expression fully reversed YTHDC1 KD-induced growth inhibition, cell apoptosis and differentiation, and colony-forming ability defect in MOLM-13 cells. MCM4 is a key subunit of the MCM2-7 complex, a putative replicative helicase involved in replication forks formation, and lack of MCM4 causes cell cycle arrest before S phase entry as well as DNA damage⁵⁵⁻⁵⁷. Interestingly, we found that YTHDC1 KD significantly blocked G1/S transition and prevented S phase entry (Figure 6L-M), and induced DNA damage, as determined by an increased expression of γ H₂AX (Figure 6N-O; supplemental Figure 8F). Proliferation cell nuclear antigen (PCNA) is a key co-factor participating in DNA replication and non-replicative DNA synthesis⁵⁸. We found that the percentage of PCNA positive cells significantly reduced in YTHDC1 KD cells, suggesting that YTHDC1 KD inhibited cell proliferation (Figure 6P-Q). Notably, restoration of MCM4 expression rescued YTHDC1

KD-induced blockage of cell proliferation and DNA damage (Figure 6L-Q; supplemental Figure 8F). Not surprisingly, MCM4 can also partially rescue the YTHDC1-KD-induced defects in cell proliferation and survival of KASUMI-1 and mouse AML cells (supplemental Figure 8G-Q). To determine the effect of YTHDC1 on DNA replication, we performed DNA fiber assay⁴¹. As shown in Figure 6R-U, the average of DNA fiber length was significantly shorter in YTHDC1 KD MOLM-13 and KASUMI-1 cells compared with the control cells, suggesting that YTHDC1 KD slows down DNA replication. Notably, MCM4 re-expression partially rescued YTHDC1 KD-induced blockage of DNA replication. Collectively, these data suggest that YTHDC1 is involved in DNA replication by regulating MCM4 expression.

To investigate whether MCM4, MCM5 or Chaf1a mediates the function of YTHDC1 in HSPCs, we re-expressed MCM4, MCM5 and Chaf1a in Ythdc1 KO Lin⁻ BM cells. To our surprise, none of these genes rescued functional defects of Ythdc1 KO HSPCs in proliferation and colony forming ability (supplemental Figure 8 R-T).

YTHDC1 KD Inhibits Growth of Primary AML Cells From Patients While Sparing Human Normal HSPCs.

We next determined the possibility of YTHDC1 serving as a therapeutic target in AML patients, we assessed the effects of YTHDC1 KD on primary cells derived from four AML patients as well as CD34⁺ cells derived from healthy individuals. In line with the results in MOLM-13, YTHDC1 KD in primary AML cells caused a dramatic inhibition of cell proliferation (Figure 7A-D, supplemental Figure 9A), but only had slight inhibition of growth

of CD34⁺ cells (Figure 7E). YTHDC1 KD significantly increased the apoptotic rate of LSC-enriched population (CD34⁺) as well as total primary AML cells but not CD34⁺ cells from healthy individuals (Figure 7F; supplemental Figure 9B-C). Moreover, YTHDC1 KD had significantly higher inhibitory effect on the colony-forming ability of primary AML cells than that of CD34⁺ cells from healthy individuals (Figure 7G). Notably, YTHDC1 KD markedly increased the frequency of CD11b⁺CD34⁻ and reduced frequency of LSC-enriched cell population (CD11b⁻CD34⁺) in YTHDC1 KD primary AML cells while marginally affected the frequency of CD11b in CD34⁺ cells from healthy donors (Figure 7H-L). As shown by morphology of the cells, there were more differentiated cells with a reduced nucleus to cytoplasm ratio in YTHDC1 KD AML cells compared to the control AML cells (Figure 7M). Consistent with observations in mouse AML cells, these results suggest that YTHDC1 KD induces differentiation of primary AML cells but shows no effect on differentiation of CD34⁺ cells from healthy individuals. To determine the effect of YTHDC1 KD on growth of human AML cells *in vivo*, MOLM-13 AML cells expressed with YTHDC1 shRNAs were transplanted into irradiated NSG mice (NOD scid gamma mouse). As shown in Figure 7N-O, the recipient mice reconstituted with YTHDC1 KD MOLM-13 cells had a significantly reduced leukemia burden and survived for a longer time compared to the mice transplanted with Scramble expressed MOLM-13 cells.

Discussion:

Here, we report a critical role of YTHDC1 in normal hematopoiesis and AML pathogenesis. Previous studies showed that reduced m⁶A methylation level as a consequence of *Mettl3/Mettl14* depletion has a moderately negative impact on HSC self-renewal while *Alkbh5* deletion-caused m⁶A upregulation does not affect HSC maintenance in the steady state^{21,23,27,29,30,59}. Loss of *Ythdf2* results in HSC and myeloid expansion²⁴⁻²⁶. In contrast, we showed that complete loss of *Ythdc1* led to bone marrow failure due to a rapid HSC exhaustion in mice (Figure 4E, L, N, and supplemental Figure 5L-M) while *Ythdc1* haploinsufficiency did not affect the survival and repopulation of HSCs in mice. Additionally, YTHDC1 KD did not significantly affect human CD34⁺ HSPC survival and proliferation either. These data suggest that *Ythdc1* is critical for HSC maintenance and normal hematopoiesis. Complete deletion of *Ythdc1* is lethal for HSPCs and a minimal amount of YTHDC1/*Ythdc1* may be sufficient for HSPC survival. However, whether YTHDC1/*Ythdc1* has a different or identical role in the maintenance of human and mouse HSPCs remains to be determined by additional studies in the future. YTHDC1, as an m⁶A reader, mediates the functional role of m⁶A methylation of nuclear RNAs. Our data demonstrate the significance of nuclear RNA m⁶A modification in normal hematopoiesis and HSC maintenance.

We found that YTHDC1 is upregulated in AML patients, and it is required for

leukemogenesis. However, we failed to detect upregulation of Ythdc1 in MLL-AF9, PML-RARA, AE9a transformed murine Lin⁻ BM cells a few days after infection (data not shown), suggesting that these oncogenes may not directly upregulate Ythdc1 gene in mouse HSPCs. Our results showed that YTHDC1 regulates DNA replication, survival and differentiation of AML cells, at least partially, through controlling the expression of the MCM4 gene, which encodes the key component of the MCM complex, in an m⁶A dependent manner. MCM4 plays a vital role in DNA replication and S phase entry^{56,57}. Upregulation of MCM4 was observed in proliferating cells, which retain the potential to become malignant. Loss of MCM4 causes DNA damage and genome instability, thereby potentially promoting cancer development^{55,60}. High MCM4 expression was founded in a variety of solid cancers, including lung triple-negative adenocarcinomas⁶¹, laryngeal squamous cell carcinoma (LSCC)⁶², ovarian cancer⁶³, and cervical cancer⁶⁴. MCM4 loss could significantly inhibit LSCC cell proliferation and induce apoptosis⁶². Mutations of MCM4 are found to be associated with different cancers⁶⁵. Here, we show that MCM4 mediates the role of YTHDC1 in leukemogenesis by regulating DNA replication and repair and cell differentiation in AML cells. In addition to MCM4, YTHDC1 also regulates expression of transcripts that encode other subunits of MCM complex including MCM2, 5, suggesting that down-regulation of MCM genes as a result of YTHDC1 KD may have a synergistic effect on MCM complex-mediated DNA replication and DNA repair. Other downstream targets of YTHDC1, as defined by global gene expression profiling, may also contribute to the function of YTHDC1 in AML cells. Taken together, our studies suggest that YTHDC1 as a nuclear m⁶A reader promotes leukemogenesis through distinct mechanisms, consolidating the concept

that m⁶A readers also have a critical role in AML pathogenesis.

Previous studies showed that YTHDC1 regulates RNA splicing, nuclear export and chromosome-associated regulatory RNA (car RNA) decay in the nucleus¹⁴⁻¹⁷. YTHDC1 can competitively bind with SRSF3 and SRSF10 to regulate mRNA splicing¹⁵. However, YTHDC1 KD in leukemia cells did not affect MCM4 splicing as determined by RNA-seq analysis (data not shown). We also demonstrated that YTHDC1 KD did not affect the nuclear export and translation efficiency of MCM4 and MCM5 in AML cells. To our surprise, we showed that YTHDC1 regulates MCM2 , 4 and 5 expression through controlling stability of these transcripts in AML cells.

Although Ythdc1 is required for survival and self-renewal of both HSCs and LSCs in mice, we found that YTHDC1 KD had a dramatic inhibition of proliferation and survival and promoted differentiation of human leukemia cell lines carrying different subtypes of chromosome abnormalities as well as primary leukemia cells, but YTHDC1 KD had minor effects on CD34⁺ human HSPCs from healthy donors. These data suggest AML blast cells with YTHDC1 overexpression likely are more sensitive to YTHDC1 inhibition compared to normal HSPCs cells. However, whether there is a therapeutic window for targeting YTHDC1 in AML patients remains to be determined by additional studies in the future.

Acknowledgments

This work was partially supported by National Institutes of Health (NIH) RO1 Grants HL131444 (Z.Q.), DK107615 (Z.Q.) and RM1 HG008935 (C.H.), Z.Q. is a Leukemia & Lymphoma Society (LLS) Scholar. S.B.-M. is a Children's Miracle Network Scholar. C.H. is an Investigator of the Howard Hughes Medical Institute (HHMI).

Authorship Contributions:

Z.Q. and C.H. conceived the project and designed the experiments. Y.S., J.W., F.Y., H.X., C.Y., Q.W., Y.L. performed experiments; Z.Q., Y.S., H.X., Y. W., L.L. and X.C. analyzed data; Z.Q. and Y.S. wrote the manuscript; B.S., X.G., W.L. and S.B.M. provided advice and new reagents/analytic tools and all authors provided critical review of the manuscript.

Conflict of interest disclosure: C.H. is a scientific founder and a scientific advisory board member of Accent Therapeutics. Inc. and a shareholder of Epican Genentech. Other authors declare no potential conflicts of interest.

References

1. Shi H, Wei J, He C. Where, When, and How: Context-Dependent Functions of RNA Methylation Writers, Readers, and Erasers. *Mol Cell*. 2019;74(4):640-650.
2. Nachtergaele S, He C. Chemical Modifications in the Life of an mRNA Transcript. *Annu Rev Genet*. 2018;52:349-372.
3. Zhao BS, Roundtree IA, He C. Post-transcriptional gene regulation by mRNA modifications. *Nat Rev Mol Cell Biol*. 2017;18(1):31-42.
4. Zaccara S, Ries RJ, Jaffrey SR. Reading, writing and erasing mRNA methylation. *Nat Rev Mol Cell Biol*. 2019;20(10):608-624.
5. Yang Y, Hsu PJ, Chen YS, Yang YG. Dynamic transcriptomic m(6)A decoration: writers, erasers, readers and functions in RNA metabolism. *Cell Res*. 2018;28(6):616-624.
6. Dominissini D, Moshitch-Moshkovitz S, Schwartz S, et al. Topology of the human and mouse m6A RNA methylomes revealed by m6A-seq. *Nature*. 2012;485(7397):201-206.
7. Wang X, Lu Z, Gomez A, et al. N6-methyladenosine-dependent regulation of messenger RNA stability. *Nature*. 2014;505(7481):117-120.
8. Wang X, Zhao BS, Roundtree IA, et al. N(6)-methyladenosine Modulates Messenger RNA Translation Efficiency. *Cell*. 2015;161(6):1388-1399.
9. Xu C, Wang X, Liu K, et al. Structural basis for selective binding of m6A RNA by the YTHDC1 YTH domain. *Nat Chem Biol*. 2014;10(11):927-929.

10. Luo S, Tong L. Molecular basis for the recognition of methylated adenines in RNA by the eukaryotic YTH domain. *Proc Natl Acad Sci U S A*. 2014;111(38):13834-13839.
11. Du H, Zhao Y, He J, et al. YTHDF2 destabilizes m(6)A-containing RNA through direct recruitment of the CCR4-NOT deadenylase complex. *Nat Commun*. 2016;7:12626.
12. Shi H, Wang X, Lu Z, et al. YTHDF3 facilitates translation and decay of N(6)-methyladenosine-modified RNA. *Cell Res*. 2017;27(3):315-328.
13. Alarcón CR, Goodarzi H, Lee H, Liu X, Tavazoie S, Tavazoie SF. HNRNPA2B1 is a mediator of m6A-dependent nuclear RNA processing events. *Cell*. 2015;162(6):1299-1308.
14. Liu J, Dou X, Chen C, et al. N (6)-methyladenosine of chromosome-associated regulatory RNA regulates chromatin state and transcription. *Science*. 2020;367(6477):580-586.
15. Xiao W, Adhikari S, Dahal U, et al. Nuclear m(6)A Reader YTHDC1 Regulates mRNA Splicing. *Mol Cell*. 2016;61(4):507-519.
16. Roundtree IA, Luo GZ, Zhang Z, et al. YTHDC1 mediates nuclear export of N(6)-methyladenosine methylated mRNAs. *Elife*. 2017;6.
17. Kasowitz SD, Ma J, Anderson SJ, et al. Nuclear m6A reader YTHDC1 regulates alternative polyadenylation and splicing during mouse oocyte development. *PLoS Genet*. 2018;14(5):e1007412.
18. Frye M, Harada BT, Behm M, He C. RNA modifications modulate gene expression during development. *Science*. 2018;361(6409):1346-1349.
19. Vu LP, Cheng Y, Kharas MG. The Biology of m(6)A RNA Methylation in Normal and Malignant Hematopoiesis. *Cancer Discov*. 2019;9(1):25-33.

20. Weng H, Huang H, Chen J. RNA N (6)-Methyladenosine Modification in Normal and Malignant Hematopoiesis. *Adv Exp Med Biol.* 2019;1143:75-93.
21. Lee H, Bao S, Qian Y, et al. Stage-specific requirement for Mettl3-dependent m(6)A mRNA methylation during haematopoietic stem cell differentiation. *Nat Cell Biol.* 2019;21(6):700-709.
22. Weng H, Huang H, Wu H, et al. METTL14 Inhibits Hematopoietic Stem/Progenitor Differentiation and Promotes Leukemogenesis via mRNA m(6)A Modification. *Cell Stem Cell.* 2018;22(2):191-205 e199.
23. Yao QJ, Sang L, Lin M, et al. Mettl3-Mettl14 methyltransferase complex regulates the quiescence of adult hematopoietic stem cells. *Cell Res.* 2018;28(9):952-954.
24. Li Z, Qian P, Shao W, et al. Suppression of m(6)A reader Ythdf2 promotes hematopoietic stem cell expansion. *Cell Res.* 2018;28(9):904-917.
25. Paris J, Morgan M, Campos J, et al. Targeting the RNA m(6)A Reader YTHDF2 Selectively Compromises Cancer Stem Cells in Acute Myeloid Leukemia. *Cell Stem Cell.* 2019;25(1):137-148 e136.
26. Wang H, Zuo H, Liu J, et al. Loss of YTHDF2-mediated m(6)A-dependent mRNA clearance facilitates hematopoietic stem cell regeneration. *Cell Res.* 2018;28(10):1035-1038.
27. Shen C, Sheng Y, Zhu AC, et al. RNA Demethylase ALKBH5 Selectively Promotes Tumorigenesis and Cancer Stem Cell Self-Renewal in Acute Myeloid Leukemia. *Cell Stem Cell.* 2020;27(1):64-80 e69.
28. Huang HL, Weng HY, Deng XL, Chen JJ. RNA Modifications in Cancer: Functions, Mechanisms, and Therapeutic Implications. *Annual Review of Cancer Biology, Vol 4.*

2020;4:221-240.

29. Vu LP, Pickering BF, Cheng Y, et al. The N(6)-methyladenosine (m(6)A)-forming enzyme METTL3 controls myeloid differentiation of normal hematopoietic and leukemia cells. *Nat Med*. 2017;23(11):1369-1376.
30. Weng H, Huang H, Wu H, et al. METTL14 Inhibits Hematopoietic Stem/Progenitor Differentiation and Promotes Leukemogenesis via mRNA m(6)A Modification. *Cell Stem Cell*. 2017.
31. Barbieri I, Tzelepis K, Pandolfini L, et al. Promoter-bound METTL3 maintains myeloid leukaemia by m(6)A-dependent translation control. *Nature*. 2017;552(7683):126-131.
32. Li Z, Weng H, Su R, et al. FTO Plays an Oncogenic Role in Acute Myeloid Leukemia as a N6-Methyladenosine RNA Demethylase. *Cancer Cell*. 2016.
33. Chen C, Liu W, Guo J, et al. Nuclear m(6)A reader YTHDC1 regulates the scaffold function of LINE1 RNA in mouse ESCs and early embryos. *Protein Cell*. 2021.
34. Kuhn R, Schwenk F, Aguet M, Rajewsky K. Inducible gene targeting in mice. *Science*. 1995;269(5229):1427-1429.
35. Shen C, Sheng Y, Zhu AC, et al. RNA Demethylase ALKBH5 Selectively Promotes Tumorigenesis and Cancer Stem Cell Self-Renewal in Acute Myeloid Leukemia. *Cell Stem Cell*. 2020;27(1):64-+.
36. Hou Y, Li W, Sheng Y, et al. The transcription factor Foxm1 is essential for the quiescence and maintenance of hematopoietic stem cells. *Nat Immunol*. 2015;16(8):810-818.
37. Sheng Y, Ma R, Yu C, et al. Role of c-Myc haploinsufficiency in the maintenance of HSCs in mice. *Blood*. 2021;137(5):610-623.

38. Sheng Y, Yu C, Liu Y, et al. FOXM1 regulates leukemia stem cell quiescence and survival in MLL-rearranged AML. *Nat Commun.* 2020;11(1):928.
39. Wang X, Spandidos A, Wang H, Seed B. PrimerBank: a PCR primer database for quantitative gene expression analysis, 2012 update. *Nucleic Acids Res.* 2012;40(Database issue):D1144-1149.
40. Dominissini D, Moshitch-Moshkovitz S, Schwartz S, et al. Topology of the human and mouse m⁶A RNA methylomes revealed by m⁶A-seq. *Nature.* 2012;485(7397):201.
41. Rageul J, Park JJ, Zeng PP, et al. SDE2 integrates into the TIMELESS-TIPIN complex to protect stalled replication forks. *Nat Commun.* 2020;11(1):5495.
42. Schneider CA, Rasband WS, Eliceiri KW. NIH Image to ImageJ: 25 years of image analysis. *Nat Methods.* 2012;9(7):671-675.
43. Tang Z, Kang B, Li C, Chen T, Zhang Z. GEPIA2: an enhanced web server for large-scale expression profiling and interactive analysis. *Nucleic Acids Res.* 2019;47(W1):W556-W560.
44. Bagger FO, Kinalis S, Rapin N. BloodSpot: a database of healthy and malignant haematopoiesis updated with purified and single cell mRNA sequencing profiles. *Nucleic Acids Res.* 2019;47(D1):D881-D885.
45. Collins CT, Hess JL. Role of HOXA9 in leukemia: dysregulation, cofactors and essential targets. *Oncogene.* 2016;35(9):1090-1098.
46. Metzger D, Clifford J, Chiba H, Chambon P. Conditional Site-Specific Recombination in Mammalian-Cells Using a Ligand-Dependent Chimeric Cre Recombinase. *Proceedings of the National Academy of Sciences of the United States of America.* 1995;92(15):6991-6995.

47. Krivtsov AV, Twomey D, Feng Z, et al. Transformation from committed progenitor to leukaemia stem cell initiated by MLL-AF9. *Nature*. 2006;442(7104):818-822.
48. Wang Y, Krivtsov AV, Sinha AU, et al. The Wnt/beta-catenin pathway is required for the development of leukemia stem cells in AML. *Science*. 2010;327(5973):1650-1653.
49. Lin S, Choe J, Du P, Triboulet R, Gregory RI. The m(6)A Methyltransferase METTL3 Promotes Translation in Human Cancer Cells. *Mol Cell*. 2016;62(3):335-345.
50. Patil DP, Chen CK, Pickering BF, et al. m(6)A RNA methylation promotes XIST-mediated transcriptional repression. *Nature*. 2016;537(7620):369-373.
51. Tye BK. MCM proteins in DNA replication. *Annu Rev Biochem*. 1999;68:649-686.
52. Shibahara K, Stillman B. Replication-dependent marking of DNA by PCNA facilitates CAF-1-coupled inheritance of chromatin. *Cell*. 1999;96(4):575-585.
53. Cortese A, Simone R, Sullivan R, et al. Biallelic expansion of an intronic repeat in RFC1 is a common cause of late-onset ataxia. *Nature Genetics*. 2019;51(4):649-+.
54. Bochman ML, Schwacha A. The Mcm Complex: Unwinding the Mechanism of a Replicative Helicase. *Microbiology and Molecular Biology Reviews*. 2009;73(4):652-683.
55. Bailis JM, Forsburg SL. MCM proteins: DNA damage, mutagenesis and repair. *Curr Opin Genet Dev*. 2004;14(1):17-21.
56. Ishimi Y. A DNA helicase activity is associated with an MCM4, -6, and -7 protein complex. *J Biol Chem*. 1997;272(39):24508-24513.
57. Maiorano D, Van Assendelft GB, Kearsey SE. Fission yeast cdc21, a member of the MCM protein family, is required for onset of S phase and is located in the nucleus throughout the cell cycle. *EMBO J*. 1996;15(4):861-872.

58. Choe KN, Moldovan GL. Forging Ahead through Darkness: PCNA, Still the Principal Conductor at the Replication Fork. *Molecular Cell*. 2017;65(3):380-392.
59. Cheng Y, Luo H, Izzo F, et al. m(6)A RNA Methylation Maintains Hematopoietic Stem Cell Identity and Symmetric Commitment. *Cell Rep*. 2019;28(7):1703-1716 e1706.
60. Ishimi Y. Regulation of MCM2-7 function. *Genes Genet Syst*. 2018;93(4):125-133.
61. Cao Y, Zhu W, Chen W, Wu J, Hou G, Li Y. Prognostic Value of BIRC5 in Lung Adenocarcinoma Lacking EGFR, KRAS, and ALK Mutations by Integrated Bioinformatics Analysis. *Dis Markers*. 2019;2019:5451290.
62. Han J, Lian M, Fang J, et al. Minichromosome maintenance (MCM) protein 4 overexpression is a potential prognostic marker for laryngeal squamous cell carcinoma. *J BUON*. 2017;22(5):1272-1277.
63. Xie L, Li T, Yang LH. E2F2 induces MCM4, CCNE2 and WHSC1 upregulation in ovarian cancer and predicts poor overall survival. *Eur Rev Med Pharmacol Sci*. 2017;21(9):2150-2156.
64. Das M, Prasad SB, Yadav SS, et al. Over expression of minichromosome maintenance genes is clinically correlated to cervical carcinogenesis. *PLoS One*. 2013;8(7):e69607.
65. Watanabe E, Ohara R, Ishimi Y. Effect of an MCM4 mutation that causes tumours in mouse on human MCM4/6/7 complex formation. *J Biochem*. 2012;152(2):191-198.

Figure Legends:

Figure 1: YTHDC1 regulates proliferation and survival of human AML cells in an m⁶A dependent manner.

(A) Comparison of the expression level of YTHDC1 in primary AML patients with healthy donor from TCGA database.

(B) Comparison of the expression level of YTHDC1 in primary AML patients bearing various chromosomal translocations with those in BM hematopoietic stem cells (HSCs) collected from healthy donors. The expression values (detected by Affymetrix exon arrays) were log2-transformed. The p value was detected by One-way ANOVA followed by multiple comparisons to HSC group. Normal: AML with normal karyotype; Complex: AML with complex karyotype.

(C) Western blot showing protein level of YTHDC1 in AML patient cells, AML cell lines and CD34⁺ cells from healthy donor.

(D) Western blot indicating knockdown efficiency of YTHDC1 by specific shRNAs in NB-4, KASUMI-1, and MOLM-13 cells.

(E-G) Growth curve of MOLM-13 (E), KASUMI-1 (F) and NB-4 (G) cells expressed Scramble shRNA (Scr), YTHDC1 shRNA1# (Ysh1#) and YTHDC1 shRNA2# (Ysh2#), cells were counted every two days.

(H) Flow cytometric analysis of apoptosis frequency of MOLM-13, KASUMI-1 and NB-4

cells expressed Scramble shRNA (Scr), YTHDC1 shRNA1# (Ysh1#) and YTHDC1 shRNA2# (Ysh2#). Annexin V⁺ indicated the apoptotic cells.

(I) Colony forming units of MOLM-13, KASUMI-1 and NB-4 cells expressed Scramble shRNA (Scr), YTHDC1 shRNA1# (Ysh1#) and YTHDC1 shRNA2# (Ysh2#). Colony number was counted 7 days after plating, 2000 cells /well for MOLM-13 and KASUMI-1 input; 1000 cells/well for NB-4 input.

(J-L) Flow cytometric analysis of differentiated cell frequency (CD11b⁺ only, CD14⁺ only and total) of MOLM-13 (J), KASUMI-1 (K) and NB-4 (L) cells expressed Scramble shRNA (Scr), YTHDC1 shRNA1# (Ysh1#) and YTHDC1 shRNA2# (Ysh2#).

*p < 0.05, **p < 0.01, ***p < 0.001, mean ± s.d., t-test.

Figure 2: *Ythdc1* is required for AML development and maintenance *in vivo*.

(A) Semiquantitative PCR analysis of Cre and the deletion of *Ythdc1*, loxP-flanked *Ythdc1* allele (loxP) and wildtype (wt) among genomic DNA in BM Lin⁻ cells from *Ythdc1*^{fl/+} (WT), *Ythdc1*^{fl/+}Mx1-Cre (*Ythdc1* HET) and *Ythdc1*^{fl/fl}Mx1-Cre (*Ythdc1* KO) mice, deletion was induced by pIpC injection.

(B-E) Growth curve of Lin⁻ BM cells from WT, *Ythdc1* HET and *Ythdc1* KO mice expressed MLL-AF9 (B), AML1-ETO9a (C), PML-Rara (D) and HOXA9 (E).

(F-G) Colony forming units of Lin⁻ BM cells from WT, *Ythdc1* HET and *Ythdc1* KO mice expressed MLL-AF9 (F), representative images of the colonies for the 3rd round (WT and HET) or 1st round (KO) of plating are displayed (G). Cells were resuspended and replated weekly in Methocult™ medium containing cytokines, bar = 100 μM.

- (H) Flow cytometric analysis of engraftment of YFP⁺ cells in peripheral blood from MLL-AF9-WT (WT), MLL-AF9-*Ythdc1* HET (HET) and MLL-AF9-*Ythdc1* KO (KO) mice 1-month post-transplantation, n = 5 mice for each group.
- (I) Complete blood count analysis of white blood cells (WBCs) in MLL-AF9-WT (WT), MLL-AF9-*Ythdc1* HET (HET) and MLL-AF9-*Ythdc1* KO (KO) mice 1-month post-transplantation, n = 5 mice for each group.
- (J) Kaplan–Meier survival analysis of MLL-AF9-WT (WT), MLL-AF9-*Ythdc1* HET (HET) and MLL-AF9-*Ythdc1* KO (KO) mice, n = 10 mice for WT group, n = 8 mice for HET group, n = 5 mice for KO group.
- (K) Wright-Giemsa-stained PB and H&E-stained spleen and liver of the MLL-AF9-WT (WT), MLL-AF9-*Ythdc1* HET (HET) and MLL-AF9-*Ythdc1* KO (KO) mice are shown. Bar = 20 μ M for PB, bar = 100 μ M for spleen and liver.
- (L) Complete blood count analysis of white blood cells (WBCs) in MLL-AF9-*Ythdc1*^{fl/fl} ER Cre mice with or without Tamoxifen (TAM) treatment, mice were injected 2 mg Tamoxifen in 100 μ L corn oil once a day for 5 consecutive days by intraperitoneal injection when the leukemia cell ratio reached to 10% up in peripheral blood, n = 5 mice for each group.
- (M) Flow cytometric analysis of apoptosis frequency of BM cells isolated from MLL-AF9-*Ythdc1*^{fl/fl} ER Cre mice with or without Tamoxifen (TAM) treatment 1-month post-administration, n = 4 mice for each group.
- (N) Wright-Giemsa-stained bone marrow (BM) and peripheral blood (PB), and H&E-stained liver of the MLL-AF9-*Ythdc1*^{fl/fl} ER Cre mice with or without Tamoxifen (TAM) treatment 1-month post-administration, bar = 10 μ M for BM and PB cells, 100 μ M for liver sections.

(O) Kaplan–Meier survival analysis of MLL-AF9-*Ythdc1*^{fl/fl} ER Cre mice with or without Tamoxifen (TAM) treatment, n = 10 mice for non-treatment group, n = 6 mice for Tamoxifen treatment group.

*p < 0.05, **p < 0.01, ***p < 0.001, mean ± s.d., t-test or Log-rank (Mantel-Cox) Test for survival curve.

Figure 3: *Ythdc1* plays a crucial role in leukemia stem cell maintenance.

(A) Flow cytometric analysis of percentage of Lin⁻ and Lin⁻cKit⁺ in MLL-AF9-WT and MLL-AF9-*Ythdc1* HET cells, which were cultured in liquid medium with cytokines for 7 days.

(B) Flow cytometric analysis of apoptosis percentage of Lin⁻cKit⁺ population from MLL-AF9-WT and MLL-AF9-*Ythdc1* HET cells.

(C) Flow cytometric analysis of percentage of L-GMP (Lin⁻c-Kit⁺Sca1⁻CD34⁺FcR-γ⁺) in BM cells from MLL-AF9-WT (MA9-WT), MLL-AF9-*Ythdc1* HET (MA9-HET) and MLL-AF9-*Ythdc1* KO (MA9-KO) leukemic mice. Mice were sacrificed at the same time point and BM cells were harvested for analysis when the mice (WT and HET) became moribund, n = 6 mice for WT and HET group, n = 4 mice for KO group.

(D-E) Flow cytometric analysis of LSC quiescence in MLL-AF9-WT (MA9-WT) and MLL-AF9-*Ythdc1* HET (MA9-HET) primary mice (E). Gating strategy was shown in D. Cells were stained with DNA Dye Hoechst and RNA Dye PyroninY. Double negative population indicated the G₀ phase/quiescence, n = 6 mice for each group.

(F) Complete blood count analysis of white blood cells (WBCs) in the secondary recipient

mice reconstituted with MLL-AF9-WT (MA9-WT) and MLL-AF9-*Ythdc1* HET (MA9-HET) BM cells from the primary recipient mice, n = 5 mice for each group.

(G) Wright-Giemsa-stained peripheral blood of the secondary MLL-AF9-WT (MA9-WT) and MLL-AF9-*Ythdc1* HET (MA9-HET) mice.

(H-I) Flow cytometric analysis of percentage of L-GMP ($\text{Lin}^- \text{c-Kit}^+ \text{Sca1}^- \text{CD34}^+ \text{FcR-}\gamma^+$) in BM cells from the secondary recipient mice reconstituted with MLL-AF9-WT (MA9-WT) and MLL-AF9-*Ythdc1* HET (MA9-HET) BM cells from the primary recipient mice (I).

Gating strategy was shown in H, n = 6 mice for each group.

(J) Flow cytometric analysis of percentage of $\text{cKit}^+ \text{Gr1}^-$ in BM cells of the secondary MLL-AF9-WT (MA9-WT) and MLL-AF9-*Ythdc1* HET (MA9-HET) mice, n = 4 mice for each group.

(K) Kaplan–Meier survival analysis of the secondary MLL-AF9-WT (MA9-WT) and MLL-AF9-*Ythdc1* HET (MA9-HET) mice, n = 8 mice for WT group, n = 10 mice for HET group.

(L-M) Flow cytometric analysis of percentage of L-GMP (L) and $\text{cKit}^+ \text{Gr1}^-$ (M) in BM cells of the MLL-AF9-*Ythdc1*^{fl/fl} ER Cre mice with or without Tamoxifen (TAM) treatment, n = 4 mice for each group.

*p < 0.05, **p < 0.01, ***p < 0.001, mean \pm s.d., t-test or Log-rank (Mantel-Cox) Test for survival curve.

Figure 4: *Ythdc1* is critical for normal hematopoiesis and HSC maintenance.

(A-D) Absolute number of white blood cells (WBC), neutrophils (NE), lymphocytes (LY),

monocytes (MO), eosinophils (EO) and basophils (BA) (A), as well as red blood cells (RBC) (B), and concentration of hemoglobin (C) and platelets (PLT) (D) in peripheral blood from *Ythdc1*^{fl/+} (WT), *Ythdc1*^{fl/+}Mx1-Cre(*Ythdc1* HET) and *Ythdc1*^{fl/fl}Mx1-Cre (*Ythdc1* KO) mice, deletion was induced by pIpC injection, n= 4 mice for WT and HET group, n = 6 mice for KO group.

(E) Kaplan–Meier survival analysis of *Ythdc1*^{fl/+} (WT), *Ythdc1*^{fl/+}Mx1-Cre (*Ythdc1* HET) and *Ythdc1*^{fl/fl}Mx1-Cre (*Ythdc1* KO) mice. The graph starts from the first day after the third pIpC injection, n= 5 mice for WT and HET group, n = 6 mice for KO group.

(F) Total BM cell number in *Ythdc1*^{fl/+} (WT), *Ythdc1*^{fl/+}Mx1-Cre (*Ythdc1* HET) and *Ythdc1*^{fl/fl}Mx1-Cre (*Ythdc1* KO) mice, n= 4 mice for WT and HET group, n = 6 mice for KO group.

(G) Histological analysis of hematoxylin and eosin-stained sternum from *Ythdc1*^{fl/+} (WT), *Ythdc1*^{fl/+}Mx1-Cre (*Ythdc1* HET) and *Ythdc1*^{fl/fl}Mx1-Cre (*Ythdc1* KO) mice, bar = 50 μ M.

(H-J) Myeloid cell (Mac⁺Gr1⁺) number (H), B cell (B220⁺) number (I) in BM and T cell number (J) in thymus in *Ythdc1*^{fl/+} (WT), *Ythdc1*^{fl/+}Mx1-Cre (*Ythdc1* HET) and *Ythdc1*^{fl/fl}Mx1-Cre (*Ythdc1* KO) mice, n= 4 mice for WT and HET group, n = 6 mice for KO group.

(K) Colony forming units of BM cells from *Ythdc1*^{fl/+} (WT), *Ythdc1*^{fl/+}Mx1-Cre (*Ythdc1* HET) and *Ythdc1*^{fl/fl}Mx1-Cre (*Ythdc1* KO) mice, cells were resuspended and replated weekly in MethocultTM medium containing cytokines, 10000 cells for 1st input, 50000 for 2nd and 3rd input.

(L-N) Number of LSK, HPCs (M) and HSC (N) in BM from *Ythdc1*^{fl/+} (WT),

Ythdc1^{fl/+}Mx1-Cre (*Ythdc1* HET) and *Ythdc1*^{fl/fl}Mx1-Cre (*Ythdc1* KO) mice. Gating strategy is shown in L. HSC: Lin⁻c-Kit⁺Sca1⁺CD48⁻CD150⁺; LSK: Lin⁻c-Kit⁺Sca1⁺; HPC:

Lin⁻cKit⁺Sca1⁻, n= 4 mice for WT and HET group, n = 3 mice for KO group.

(O) Flow cytometric analysis of the percentage of donor-derived cells in the 1st round and 2nd round of recipient mice. pIpC was injected 1 month after transplantation, n = 4 mice for each group.

(P) Flow cytometric analysis of the percentage of donor-derived myeloid cells, B and T cells in PB in the 1st round and 2nd round of recipient mice 4 months after transplantation, n = 4 mice for each group.

(Q) Flow cytometric analysis of the percentage of donor-derived cell populations in BM in 1st round and 2nd round of recipient mice, n = 4 mice for each group.

*p < 0.05, **p < 0.01, ***p < 0.001, mean ± s.d., t-test or Log-rank (Mantel-Cox) Test for survival curve.

Figure 5: YTHDC1 regulates expressions of MCM genes by stabilizing their mRNAs.

(A) Volcano plot showing fold changes for differentially expressed genes in MOLM-13 cells expressed Scramble shRNA, YTHDC1 shRNA1# and YTHDC1 shRNA2#. The cells were collected 2-3 days after viral infection when different cell groups had a similar viability. The experiments were performed in duplicate.

(B-C) The bar graph showing the pathways significantly affected in YTHDC1 knockdown MOLM-13 cells. Down-regulated pathways were shown in B and up-regulated pathways were shown in C. RNA-seq analysis was performed using Partek® Flow® software.

- (D) Analysis of RNA-seq data, m⁶A-seq and YTHDC1 RIP-seq data to define YTHDC1 direct target genes.
- (E) Quantitative RT-PCR validation of the selected target genes in MOLM-13 cells expressed Scramble shRNA (Scr), YTHDC1 shRNA1# (Ysh1#) and YTHDC1 shRNA2# (Ysh2#).
- (F) mRNA m⁶A methylation analyses of selected target genes (MCM2, MCM4, MCM5, CHAF1A and BCL2) by MeRIP assay in MOLM-13 cells.
- (G) YTHDC1-RIP analyses showing YTHDC1 enrichments at mRNAs of the selected target genes in MOLM-13 cells.
- (H) mRNA m⁶A methylation analyses of selected target genes (MCM2, MCM4, MCM5, CHAF1A and BCL2) by MeRIP assay in MOLM-13 cells expressed Scramble shRNA (Scr), YTHDC1 shRNA1# (Ysh1#) and YTHDC1 shRNA2# (Ysh2#).
- (I) YTHDC1-RIP analysis of YTHDC1 enrichments at mRNAs of the selected target genes in MOLM-13 cells expressed Scramble shRNA (Scr), YTHDC1 shRNA1# (Ysh1#) and YTHDC1 shRNA2# (Ysh2#).
- (J-K) mRNAs half-life of the selected target genes (MCM2 and MCM4) in MOLM-13 cells with, or without YTHDC1 knockdown. The p value was detected by One-way ANOVA followed by multiple comparisons to Scr group 16 hours after actinomycin D treatment.
- *p < 0.05, **p < 0.01, ***p < 0.001, mean ± s.d., t-test. Experiments were performed in triplicate and were repeated at least twice.

Figure 6: MCM4 mediates YTHDC1 functions in AML cells

- (A) Comparison of the expression level of MCM4 in primary AML patients bearing various

chromosomal translocations with those in BM hematopoietic stem cells (HSCs) collected from healthy donors. The expression values (detected by Affymetrix exon arrays) were log2-transformed. The p value was detected by One-way ANOVA followed by multiple comparisons to HSC group. Normal: AML with normal karyotype; Complex: AML with complex karyotype.

(B) Growth curve of MOLM-13 cells expressed Scramble shRNA (Scr), MCM4 shRNA1# (M4sh1#) and MCM4 shRNA2# (M4sh2#), cells were counted every two days. The p value was detected by One-way ANOVA followed by multiple comparisons to Scr group at Day 7.

(C) Flow cytometric analysis of apoptosis frequency of MOLM-13 cells expressed Scramble shRNA (Scr), MCM4 shRNA1# (M4sh1#) and MCM4 shRNA2# (M4sh2#). Annexin V⁺ indicated the apoptotic cells.

(D) Flow cytometric analysis of differentiated cell frequency of MOLM-13 expressed Scramble shRNA (Scr), MCM4 shRNA1# (M4sh1#) and MCM4 shRNA2# (M4sh2#).

(E) Colony forming units of MOLM-13 cells expressed Scramble shRNA (Scr), MCM4 shRNA1# (M4sh1#) and MCM4 shRNA2# (M4sh2#). Colony number was counted after 7 days of plating.

(F) Quantitative RT-PCR analysis of MCM4 expression in MOLM-13 cells expressed empty vector control, YTHDC1 wildtype (YTHDC1 wt) or YTHDC1 W377A W428A mutant (YTHDC1 mut).

(G) The mRNA half-life($t_{1/2}$) of MCM4 in MOLM-13 cells expressed empty vector control, YTHDC1 wildtype (YTHDC1 wt) or YTHDC1 W377A W428A mutant (YTHDC1 mut). The p value was detected by t-test between vector and YTHDC1 wt or YTHDC1 wt and mut 8

hour after actinomycin D treatment.

(H) Cell growth curve of MOLM-13 cells expressed Scramble shRNA (Scr) or YTHDC1 shRNA2# (Ysh2#) with or without MCM4 expression. The p value was detected by t-test between Scr+vector and Ysh2#+vector or Ysh2#+vector and Ysh2#+MCM4 at Day 7.

(I) Flow cytometric analysis of apoptosis frequency of MOLM-13 cells expressed Scramble shRNA (Scr) or YTHDC1 shRNA2# (Ysh2#) with or without MCM4 expression.

(J) Flow cytometric analysis of differentiated cell frequency of MOLM-13 cells expressed Scramble shRNA (Scr) or YTHDC1 shRNA2# (Ysh2#) with or without MCM4 expression.

(K) Colony forming units of MOLM-13 cells expressed Scramble shRNA (Scr) or YTHDC1 shRNA2# (Ysh2#) with or without MCM4 expression.

(L-M) Flow cytometric analysis of cell cycle in MOLM-13 cells expressed Scramble shRNA (Scr) or YTHDC1 shRNA2# (Ysh2#) with or without MCM4 expression (M). Gating strategy was shown in L. Cells were stained with BrdU (determine the S phase) and DAPI (determine the DNA content).

(N) Flow cytometric analysis of the percentage of p- γ H2AX⁺ cells in MOLM-13 cells expressed Scramble shRNA (Scr) or YTHDC1 shRNA2# (Ysh2#) with or without MCM4 expression.

(O) Western blot analysis of p- γ H2AX expression in MOLM-13 cells expressed Scramble shRNA (Scr), YTHDC1 shRNA1# (Ysh1#) or YTHDC1 shRNA2# (Ysh2#) with or without MCM4 expression. ACTIN was served as an inner control.

(P-Q) Flow cytometric analysis of the percentage of PCNA⁺ cells in MOLM-13 cells expressed Scramble shRNA (Scr) or YTHDC1 shRNA2# (Ysh2#) with or without MCM4

expression. Gating strategy was shown in P.

p < 0.01, *p < 0.001, mean \pm s.d., t-test.

(R) DNA fiber assay. Distributions of the IdU track length were determined on IdU labeled DNA fibers from MOLM-13 cells expressed Scramble shRNA (Scr) or YTHDC1 shRNA2# (Ysh2#) with or without MCM4 expression.

(S) The IdU track length of three different groups were compared. (****P < 0.0001, Mann–Whitney test). Mean lines in the boxes indicate the median value of at least 150 tracks per experimental condition. Scale bar = 5 μ m.

(T) DNA fiber assay. Distributions of the IdU track length were determined on IdU labeled DNA fibers from KASUMI-1 cells expressed Scramble shRNA (Scr) or YTHDC1 shRNA2# (Ysh2#) with or without MCM4 expression.

(U) The IdU track length of three different groups were compared. (****P < 0.0001, Mann–Whitney test). Mean lines in the boxes indicate the median value of at least 80 tracks per experimental condition. Scale bar = 5 μ m.

Figure 7: YTHDC1 KD inhibits leukemic potentials of human primary AML cells.

(A-E) Growth curve of primary AML cells from four different patients (A, B, C, D) and CD34⁺ cells (E) from healthy donors expressed Scramble shRNA (Scr), YTHDC1 shRNA1# (Ysh1#) and YTHDC1 shRNA2# (Ysh2#). CD34⁺ cells are mixed cells from three healthy donors. The experiments were performed in triplicate. The p value was detected by One-way ANOVA followed by multiple comparisons to Scr group at Day 10 (for patient cells) or Day 7 (for CD34⁺ cells).

(F) Flow cytometric analysis of apoptosis frequency of CD34⁺ cells in AML patients and CD34⁺ cells from healthy donor expressed Scramble shRNA (Scr), YTHDC1 shRNA1# (Ysh1#) and YTHDC1 shRNA2# (Ysh2#).

(G) Colony forming units of AML patient cells and CD34⁺ cells from healthy donor expressed Scramble shRNA (Scr), YTHDC1 shRNA1# (Ysh1#) and YTHDC1 shRNA2# (Ysh2#). 50000 cells/well for patient cell input, 2500 cells/well for healthy donor CD34⁺ cell input.

(H-M) Flow cytometric analysis of differentiated cell frequency of AML patient cells (H, I, J) and CD34⁺ (L) cells from healthy donor expressed Scramble shRNA (Scr), YTHDC1 shRNA1# (Ysh1#) and YTHDC1 shRNA2# (Ysh2#). Gating strategy was shown in K and wright-Giemsa-stained AML cell morphology was shown in M, differentiated cells were indicated by red arrow in M, bar = 20 μ M.

(N) Flow cytometric analysis of the percentage of human leukemia cells (CD45⁺) in NSG mice transplanted MOLM-13 cells expressed Scramble shRNA (Scr), YTHDC1 shRNA1# (Ysh1#) and YTHDC1 shRNA2# (Ysh2#).

(O) Kaplan-Meier survival analysis of MOLM-13 cells expressed Scramble shRNA (Scr), YTHDC1 shRNA1# (Ysh1#) and YTHDC1 shRNA2# (Ysh2#).

* $p < 0.05$, ** $p < 0.01$, *** $p < 0.001$, mean \pm s.d., t-test or Log-rank (Mantel-Cox) Test for survival curve. Experiments were performed in triplicate.

Figure 1

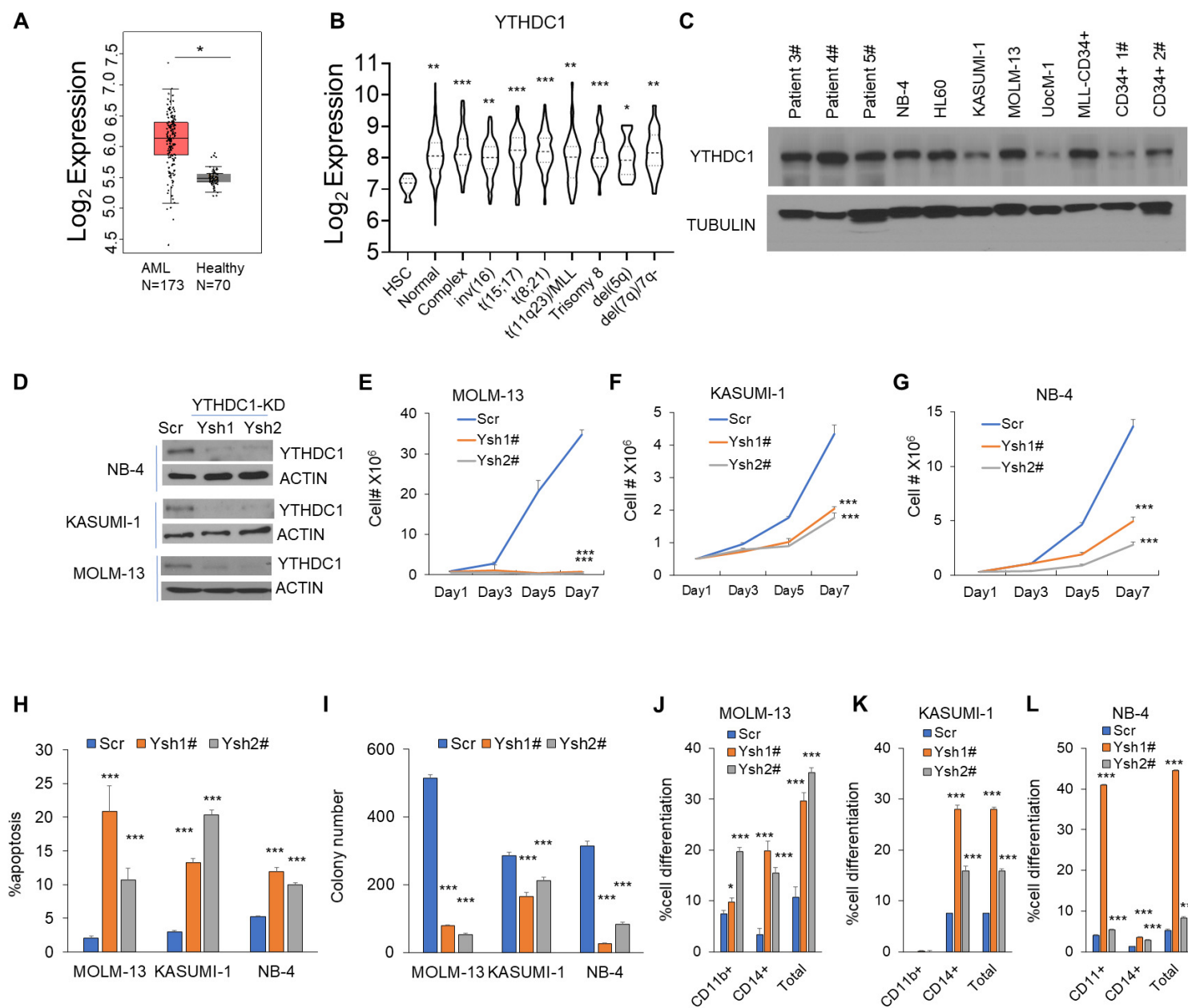


Figure 2

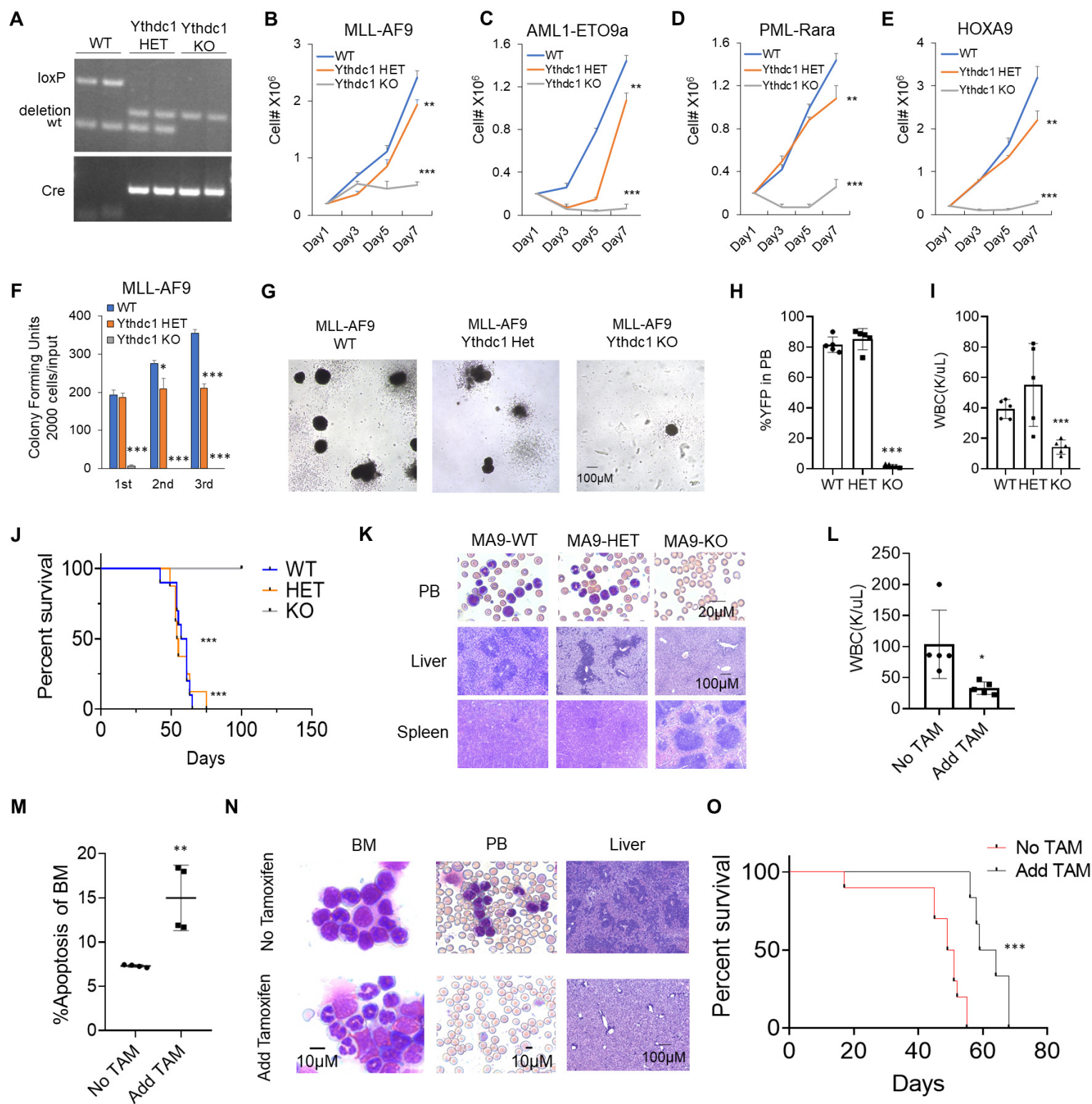


Figure 3

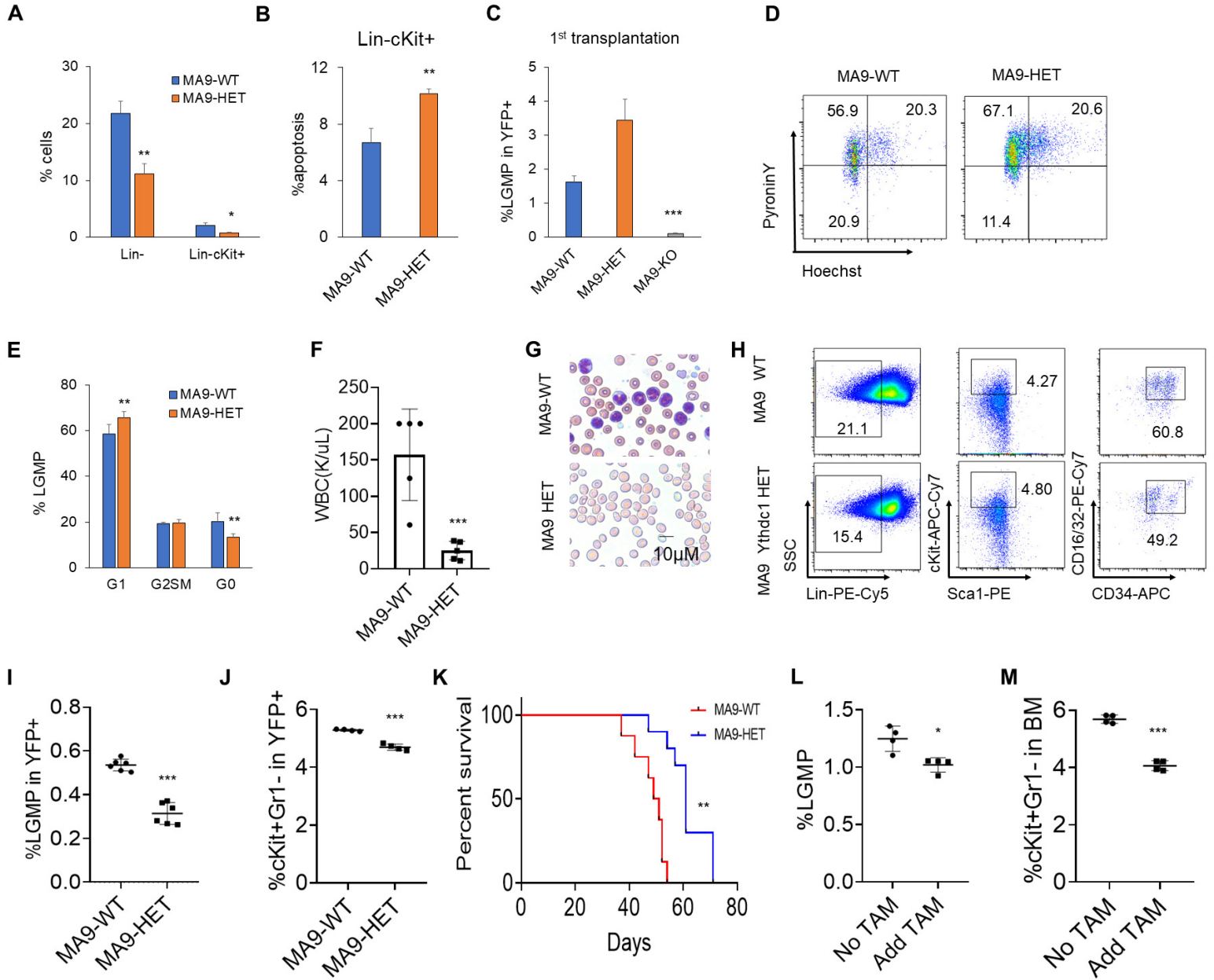


Figure 4

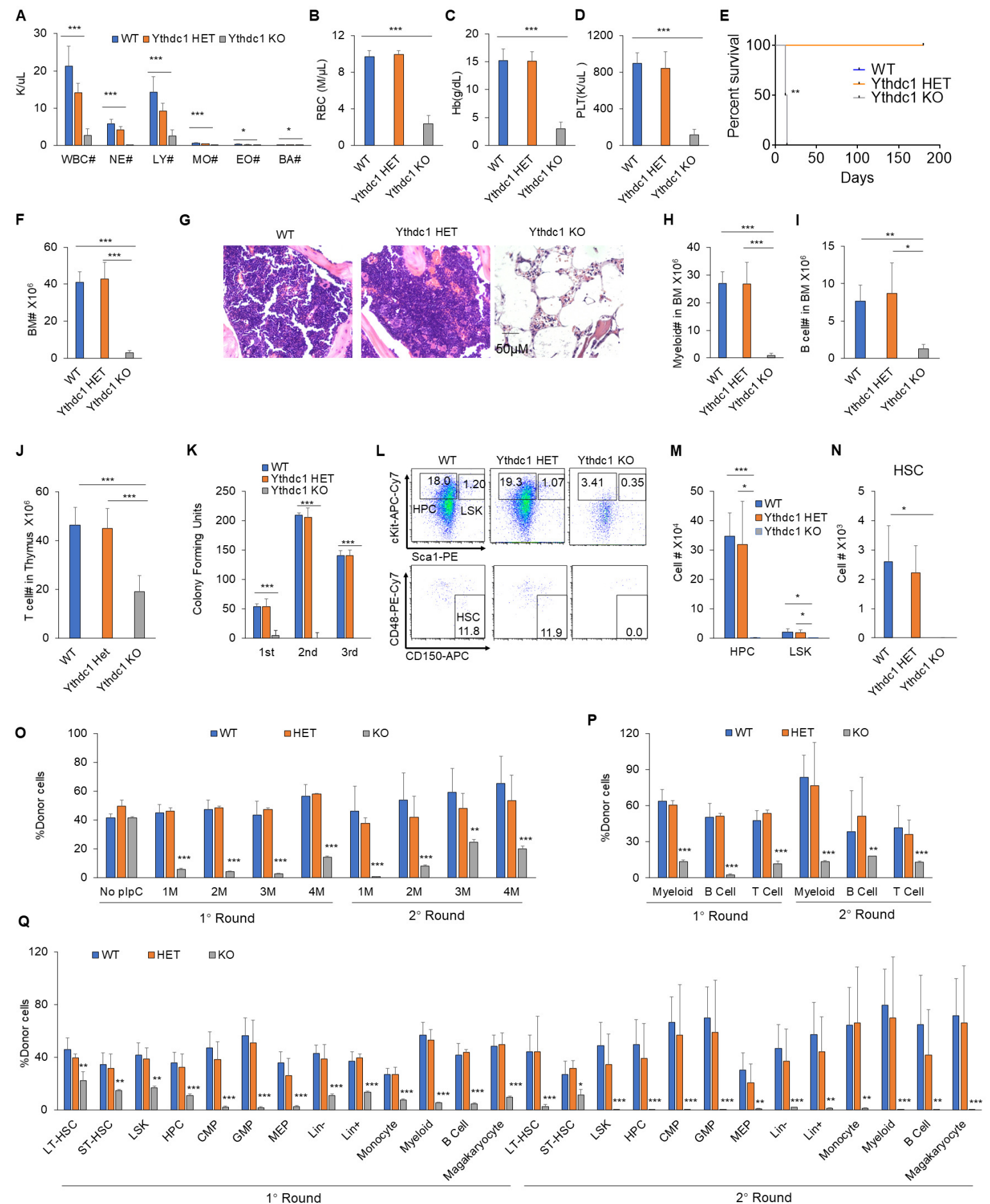


Figure 5

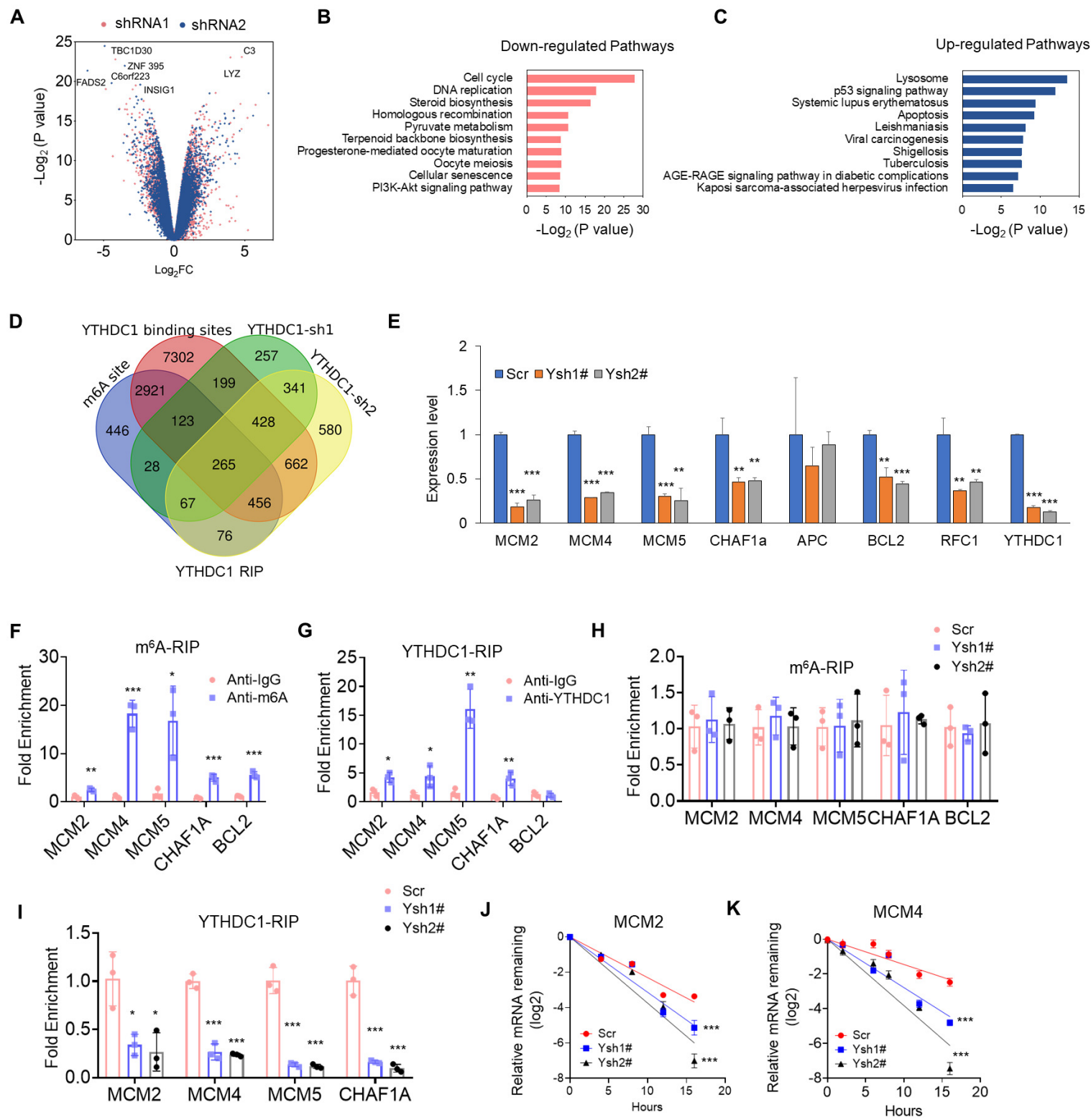


Figure 6

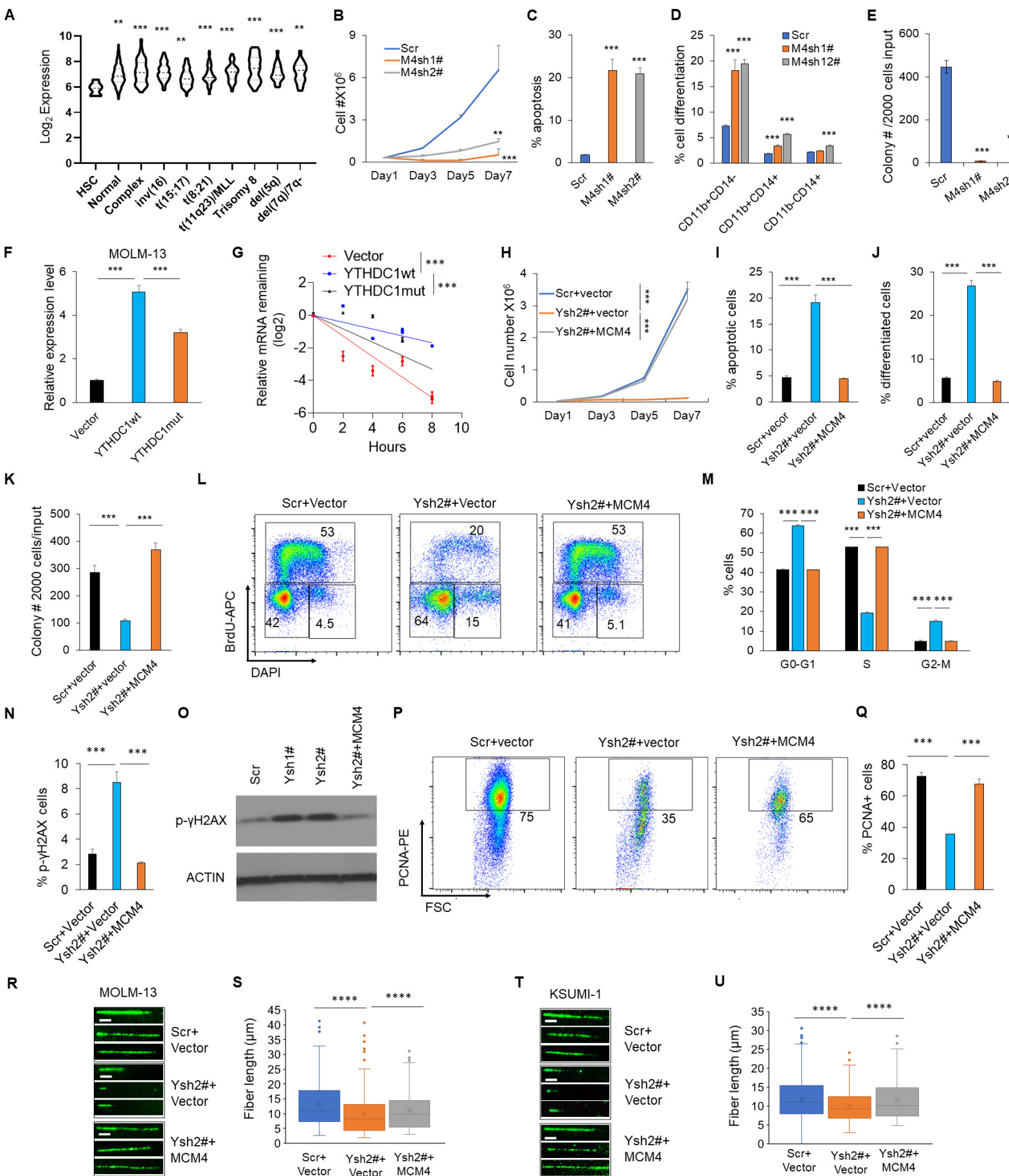


Figure 7

